

Prompt-OT: An Optimal Transport Regularization Paradigm for Knowledge Preservation in Vision-Language Model Adaptation

Xiwen Chen^{1*} Wenhui Zhu^{2*} Peijie Qiu^{3*} Hao Wang¹ Huayu Li⁴

Haiyu Wu⁵ Aristeidis Sotiras³ Yalin Wang² Abolfazl Razi¹

¹ Clemson University, ² Arizona State University, ³ Washington University in St. Louis,

⁴ University of Arizona, ⁵ University of Notre Dame

Abstract

Vision-language models (VLMs) such as CLIP demonstrate strong performance but struggle when adapted to downstream tasks. Prompt learning has emerged as an efficient and effective strategy to adapt VLMs while preserving their pre-trained knowledge. However, existing methods still lead to overfitting and degrade zero-shot generalization. To address this challenge, we propose an optimal transport (OT)-guided prompt learning framework that mitigates forgetting by preserving the structural consistency of feature distributions between pre-trained and fine-tuned models. Unlike conventional point-wise constraints, OT naturally captures cross-instance relationships and expands the feasible parameter space for prompt tuning, allowing a better trade-off between adaptation and generalization. Our approach enforces joint constraints on both vision and text representations, ensuring a holistic feature alignment. Extensive experiments on benchmark datasets demonstrate that our simple yet effective method outperforms existing prompt learning strategies in base-to-novel generalization, cross-dataset evaluation, and domain generalization, without requiring additional augmentation or ensemble techniques. The code is available at <https://github.com/ChongQingNoSubway/Prompt-OT>

1. Introduction

Foundational vision-language models (VLMs), such as CLIP [30] and ALIGN [15], trained on large-scale datasets to align image-text pairs, have demonstrated exceptional generalization capabilities across a variety of downstream tasks [8, 18, 23]. However, recent studies have shown that VLMs face challenges in maintaining generalization when adapted to downstream tasks via *e.g.* fine-tuning [17], particularly for tasks with limited samples such as few-shot learning.

*These authors contributed equally to this paper

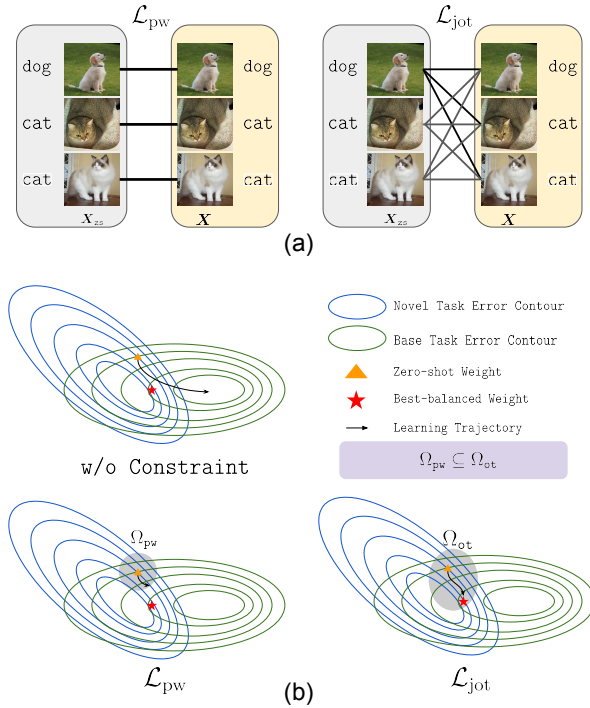


Figure 1. (a) Comparison of point-wise constraints vs. our OT-based constraints: Unlike rigid point-wise alignment, our loss captures cross-instance relationships, effectively modeling correlations both within and between classes. (b) The error contours for base and novel tasks without constraint (top left), with point-wise constraint (bottom left), and our OT-based constraints (bottom right). Our OT-based constraint enlarges feasible parameter domains, striking a balance between adaptation and generalization.

To tackle this issue, recent studies [43, 44] have shown that introducing learnable prompt tokens while keeping the original pre-trained weights fixed is an effective strategy for fine-tuning VLMs on downstream tasks (*a.k.a. Prompt Learning*). Following this trend, many efforts have been devoted to exploring different prompt learning strategies,

either through the text branch alone [43, 44] or through both the text and image branches [16, 41]. However, early prompt learning methods [16, 43, 44] often lead to overfitting in task-specific datasets and sacrifice zero-shot generalization. To address this limitation, more recent studies [17, 34] introduce explicit regularization to maintain the feature consistency between the finetuned and the frozen pre-trained (*i.e.* zero-shot) VLMs. These methods mainly employ a point/sample-wise metric (*e.g.* MSE/MAE) for the feature alignment between the zero-shot and finetuned models.

Despite this, we argue that this may not be an optimal way to impose the aforementioned feature consistency due to the following reasons: **(i)** Point-wise constraints may fail to capture cross-instance relationships, limiting their ability to account for the geometry of the underlying manifold and effectively model both within-class and cross-class relations. **(ii)** Point-wise constraints might be too restrictive¹, as different features and samples have different importance. This may cause the features to learn from prompted VLM to be shrunk to a narrow searching space. This limitation can hinder both adaptation and generalizability.

To address these challenges, we propose an optimal transport (OT)-guided VLMs prompt tuning method, which leverages OT to mitigate knowledge forgetting between the embedding features of the zero-shot and the finetuned VLMs. The advantages of OT-guided prompts are multi-fold. First, OT naturally captures cross-instance relationships, since the transport map establishes an interactive coupling among instances by redistributing mass based on their mutual relationships. Second, we prove that OT expands the feasible domain for learnable prompt tokens. A broader feasible domain introduces more potential local minima, provides greater flexibility for the optimizer to explore, and allows easier hyperparameter adjustment, increasing the likelihood of achieving an optimal balance between adaptation and generalization. The conceptual illustration is shown in Fig. 1. Third, existing methods often constrain vision and text representations independently and then combine them with a weighted sum of losses. However, the vision encoder outputs features of size $B \times d$ (where B and d denote the batch size and the latent dimension, respectively), while the text encoder outputs features of size $C \times d$ (where C denotes the number of classes). This mismatch can lead to imbalanced constraint strength across modalities. To address this, we build on the fundamental concept of an instance in CLIP, which inherently couples both vision and text. Our design therefore enforces constraints on vision and text simultaneously at the instance level, ensuring more balanced and structurally consistent multimodal representations. Consequently, our design enforces constraints on both modalities

simultaneously for each instance. It is also worth noting that, despite its simple yet effective design, our method outperforms several recent competitive approaches without relying on additional components such as ensemble methods or data augmentation techniques. In summary, our work makes the following key contributions:

- We propose an OT-based constraint scheme to mitigate knowledge forgetting, addressing the core limitations of previous constraint-based prompt learning methods. Beyond the conceptual design, we provide a *theoretical justification* showing that OT enlarges the feasible parameter space of learnable prompts, thereby enabling a more flexible and principled trade-off between adaptation and generalization.
- We propose to impose the OT constraint jointly on vision and text features of each instance. This *balances the constraint strength across modalities* and preserves structural consistency in multimodal representations, addressing the limitations of treating modalities independently.
- Empirical analysis (Table 4) highlights that *Prompt-OT* *consistently outperforms all point-wise constraint methods with statistical significance*. Across three popular benchmarks (Base-to-Novel Generalization, Cross-Dataset Evaluation, and Domain Generalization), our method achieves competitive or superior performance compared to recent approaches, including PLOT [2], PromptSRC [17], TCP [41], and QMaPLe [11], without relying on prompt ensembles or extra augmentation.

2. Related Work

Adaptation to Downstream tasks. Two popular ways to adapt a model for downstream tasks are full fine-tuning and linear probing. However, full fine-tuning can weaken generalization, while linear probing often yields poor performance, leading to both being problematic for tasks needing accuracy and generalization, like open-vocabulary image recognition and object detection [16]. To address this, researchers add extra learnable components without altering the original pre-trained weights, attempting to preserve both performance and generalization [44]. One representative approach is known as *prompt-based methods* [41, 43–45]. In these methods, the pre-trained model is adapted by incorporating a small number of learnable prompt tokens into the original input. For example, CoOp [44], CoCoOp [43], ProdGrad [45], TCP [41] introduced a set of learnable continuous vectors into the text input. Although there are some attempts to only include prompt tokens on the image branch, more recent works prefer to perform prompt learning on both branches jointly, such as MaPLe [16] and PromptSRC [17]. Instead, adapter-based methods often add some extra layers to refine features generated by CLIP [10, 40, 42].

Consistency-based Learning. Instead of focusing on the

¹A similar conclusion is also drawn in a well-known work [19] for related tasks. We have more discussion for this method in Sec. 2.

design of the architecture, there are methods to enforce consistency between the trainable and pre-trained models, thereby reducing overfitting and forgetting during downstream task fine-tuning. ProGrad [45] aligns gradient directions with the pre-trained model, while PromptSRC [17] imposes consistency on both embeddings and logits. A similar idea in [34] employs adapters, data augmentations, and LLM knowledge. *Though PromptSRC is closest to our method, it only applies pairwise constraints that match average embedding distributions. We argue this is too restrictive and overlooks structural information, as discussed in Sec. 3.3.* A related work [19] in continual learning attempts to solve severe restriction issues through a Fisher Information-based constraint, while it requires a substantial approximation during computing and needs the corresponding weights on the frozen model, which makes it infeasible for our case, as the prompt tokens are only added to the adapted model. *Additionally, previous methods typically involve terms that constrain each modality independently.* However, during CLIP training, the feature spaces of the two modalities are inherently imbalanced: the image encoder produces a $B \times d$ feature map, while the text encoder outputs a fixed $C \times d$ representation. *This discrepancy leads to uneven constraint strength across modalities.* To address this, we propose imposing constraints directly on the joint representation of each instance, ensuring better alignment. A detailed analysis is provided in Sec. 5 and Table 5.

Optimal Transport for VLMs. Some recent studies also use OT to improve learning on CLIP, such as PLOT [2], Dude [25], and AWT [46]. PLOT employs multiple learnable text prompts and uses OT to align text and vision features. Dude leverages unbalanced OT to match class-specific and domain-shared text features (augmented by an LLM) with visual features. AWT, designed for zero-shot learning, applies various image transformations and LLM-augmented text prompts, then uses OT to measure the distance between an input image and candidate labels. *Different from those methods, which typically use OT with augmented inputs to align vision and text features, our method applies OT as a regularization to align the vision-text joint distributions of the pre-trained and adapted models, without any need for augmentation.*

Augmentation for VLMs. Several recent studies introduce extra augmentation to boost VLMs' adaptation. For example, [17, 41] use more hand-crafted text templates beyond "a photo of a [category]" or design their prompts, while [34, 46] leverage LLMs for diverse semantic prompts. Others [9] rely on Stable Diffusion [33] to generate multi-view images for better test-time tuning. These methods show that high-quality augmentation can significantly improve performance on downstream tasks. *However, not everyone can access such data-augmentation resources. Thus, our method is designed to work without any extra augmentation, yet still*

delivers competitive results.

3. Method

3.1. Preliminaries

We first briefly present the basic pipeline of CLIP as well as the principle of *Prompt Learning*.

Vision Encoding. An image I is first divided into M patches and then projected to latent space, which is denoted as $\mathbf{V}^0 = \{\mathbf{v}_1^0, \dots, \mathbf{v}_M^0\}$. Afterward, a learnable class token \mathbf{v}_{cls}^0 is concatenated as the global representation, denoted as $[\mathbf{V}^0, \mathbf{v}_{cls}^0]$. These tokens are subsequently fed into a sequence of transformer blocks: $[\mathbf{V}^l, \mathbf{v}_{cls}^l] = \text{Trans}_{\text{vision}}^l([\mathbf{V}^{l-1}, \mathbf{v}_{cls}^{l-1}])$, Where $l = 1, \dots, L_I$ and L_I denote the number of vision transformer blocks in the image encoder of CLIP. Afterward, the final image representation in V-L space is obtained through an additional linear projection: $\mathbf{h} = f_{\text{visionProj}}(\mathbf{v}_{cls}^{L_I})$.

Text Encoding. Each text prompt is tokenized to N tokens, denoted as $\mathbf{T}^0 = \{\mathbf{t}_1^0, \dots, \mathbf{t}_N^0\}$. Likewise, these tokens are then fed to text transformer blocks as $\mathbf{T}^l = \text{Trans}_{\text{Text}}^l(\mathbf{T}^{l-1})$, Where $l = 1, \dots, L_T$ and L_T denote the number of transformer blocks in the text encoder of CLIP. Similarly, the final representation is obtained by the last token through a linear projection as $\mathbf{g} = f_{\text{TextProj}}(\mathbf{t}_N^{L_T})$.

Prediction. In a standard setting of zero-shot classification [16], the text encoder generates the hand-crafted text prompt using the common template "a photo of a [category]". Given class labels $y \in \{1, \dots, C\}$, we can obtain the text embedding for each class by filling out the template with the corresponding class name as $(\mathbf{g})_y$. As mentioned earlier, we also obtained the image representation for an image as \mathbf{h} . The prediction can be performed as:

$$p(\bar{y}|I) = \frac{\exp(\text{sim}(\mathbf{h}, \mathbf{g}_y)/\tau)}{\sum_{k=1}^C \exp(\text{sim}(\mathbf{h}, \mathbf{g}_k)/\tau)}, \quad (1)$$

where $\text{sim}(\cdot, \cdot)$, τ denote the cosine similarity and a pre-defined temperature, respectively.

Prompt Learning. Now, we will delve into how to perform prompt learning, which often appends some learnable tokens to text or vision branches as part of transformer layers. Formally, we denote $\mathcal{S}_{\text{vision}}$ and $\mathcal{S}_{\text{text}}$ as the layers to integrate learnable prompt tokens for the vision encoder and text encoder, respectively. We can denote the K_I vision prompt tokens and K_T text prompt tokens at $(l+1)$ -th block as $\mathbf{P}^l = \{\mathbf{p}_1^l, \dots, \mathbf{p}_{K_I}^l\}$ and $\mathbf{Q}^l = \{\mathbf{q}_1^l, \dots, \mathbf{q}_{K_T}^l\}$, respectively. The prompting for vision encoder in l -th layer ($l \in \mathcal{S}_{\text{vision}}$) can be then presented as:

$$[_, \mathbf{V}^l, \mathbf{v}_{cls}^l] = \text{Trans}_{\text{vision}}^l([\mathbf{P}^{l-1}, \mathbf{V}^{l-1}, \mathbf{v}_{cls}^{l-1}]), \quad (2)$$

and for text encoder in l -th layer ($l \in \mathcal{S}_{\text{text}}$) can be then presented as:

$$[_, \mathbf{T}^l] = \text{Trans}_{\text{text}}^l([\mathbf{Q}^{l-1}, \mathbf{T}^{l-1}]). \quad (3)$$

It is worth mentioning that this is known as *Independent Vision-Language Prompting* (IVLP), if \mathbf{P}^l and \mathbf{Q}^l are defined independently. This is used in [17, 31], and we will also use this baseline in our framework, following [17]. MaPLE [16] imposes an additional linear layer to share the knowledge between \mathbf{P} and \mathbf{Q} . In order to adapt classification on a downstream dataset, we can simply update the prompt tokens via cross-entropy loss \mathcal{L}_{CE} between predictions (Eq. 1) and ground truth labels.

3.2. Vision-Text Joint Optimal Transport

In this section, we will delve into the design of our framework. During training, this framework involves a CLIP with learnable prompts, i.e., the adapted model and a frozen pre-trained CLIP, while during inference, we only need the adapted CLIP.

As discussed in Sec. 2, constraining each modality separately can result in uneven constraint strength due to inherent imbalances. To address this, we emphasize a key principle of CLIP: *each instance is jointly represented in both the text and image domains*. Consequently, the two modalities should be constrained simultaneously at the instance level. Suppose we have a dataset $\mathcal{D} = \{(I_i, y_i)\}_{i=1}^n$, where I_i , y_i , and n denote the i th input image, its corresponding label, and the number of samples, respectively. For each instance $i \in [n]$, the vision representation is obtained by the vision encoder as \mathbf{h}^i . Since the real text caption for the image is often unknown, we use the standard template with its category as the proxy, and accordingly, we can obtain the text representation as \mathbf{g}^i . For simplicity, we concatenate both representations as the joint representation of an instance i , denoted as $\mathbf{x}_i = \text{concat}(\mathbf{h}^i, \mathbf{g}^i)$. Now, we have the distribution of joint representation of the dataset \mathcal{D} as $\mathcal{X} = \{\mathbf{x}^i\}_{i=1}^n$ by the adapted model. We also need to obtain the joint representation distribution using an additional CLIP model, i.e., the CLIP model with its original pre-trained weights, while keeping all parameters frozen. We denote it as $\mathbf{X}_{zs} = \{\mathbf{x}_{zs}^i\}_{i=1}^n$. It is worth mentioning that \mathbf{x}^i and \mathbf{x}_{zs}^i are obtained from the same input instance (I_i, y_i) , while with different CLIP models (i.e., one keeps updating and one is frozen). Our proposed regularization term is presented as follows: Given \mathbf{X} and \mathbf{X}_{zs} , the proposed constraint lies in Optimal Transport [36] is defined as:

$$\mathcal{L}_{\text{jot}}(\mathbf{X}, \mathbf{X}_{zs}) = \min_{\gamma \in \mathcal{U}(\mathbf{a}, \mathbf{b})} \sum_{i=1}^n \sum_{j=1}^n \gamma_{ij} c(\mathbf{x}^i, \mathbf{x}_{zs}^j), \quad (4)$$

where $c(\mathbf{x}^i, \mathbf{x}_{zs}^j)$ denotes a cost function (e.g. linear and quadratic cost) between \mathbf{x}^i and \mathbf{x}_{zs}^j . γ denotes a transport

map, $\mathcal{U}(\mathbf{a}, \mathbf{b})$ denotes set of all valid transport maps,

$$\mathcal{U}(\mathbf{a}, \mathbf{b}) = \{\gamma \in \mathbb{R}_+^{n \times n} \mid \gamma \mathbf{1}_n = \mathbf{a}, \gamma^\top \mathbf{1}_n = \mathbf{b}\}, \quad (5)$$

$$\mathbf{a} = \frac{1}{n} \mathbf{1}_n, \quad \mathbf{b} = \frac{1}{n} \mathbf{1}_n,$$

and $\mathbf{1}_n$ is an n -dimensional vector of ones.

In summary, this proposed loss aims to *preserve the consistency between updated joint representation and zero-shot representation while offering a larger search feasible domain of prompts and taking cross-instance from the same class or different class into consideration*. Below, we will provide a detailed analysis with theoretical justification.

3.3. Theoretical Analysis

Modeling cross-instance correlations can potentially characterize both within-class relations and between-class relations. Under the proposed OT-based constraint, each element in the transport map γ represents the amount of mass transported between two instances from the zero-shot representation and adapted representation. The learned transport map inherently captures cross-instance correlations because OT enforces a structured assignment, where similar instances are mapped with lower cost while maintaining the geometry of the data distribution. This process happens automatically because OT optimizes the movement of probability mass, ensuring that within-class relations remain compact while between-class relations reflect meaningful transitions, ultimately shaping a well-organized feature space. Here, we focus more on how using OT-loss can potentially enlarge the feasible parameter space, which potentially results in easier optimization and better convergence. We first give a general definition of the loss of point-wise constraint. Given \mathbf{X} and \mathbf{X}_{zs} , the point-wise constraint is defined as:

$$\mathcal{L}_{\text{pw}}(\mathbf{X}, \mathbf{X}_{zs}) = \frac{1}{n} \sum_{i=1}^n c(\mathbf{x}^i, \mathbf{x}_{zs}^i). \quad (6)$$

We observe that it can be presented in a similar form of optimal transport:

$$\mathcal{L}_{\text{pw}}(\mathbf{X}, \mathbf{X}_{zs}) = \sum_{i=1}^n \sum_{j=1}^n \hat{\gamma}_{ij} c(\mathbf{x}^i, \mathbf{x}_{zs}^j), \quad (7)$$

where $\forall i \neq j, \hat{\gamma}_{ij} = 0$ and $\forall i = j, \hat{\gamma}_{ij} = 1/n$.

Lemma 1. *Let \mathbf{X}_{zs} be a zero-shot representation distribution and $\epsilon > 0$ be a tolerance of the constraint. Suppose there exists a set \mathcal{X}_{pw} such that for all $\mathbf{X} \in \mathcal{X}_{\text{pw}}$, $\mathcal{L}_{\text{pw}}(\mathbf{X}, \mathbf{X}_{zs}) \leq \epsilon^2$. Similarly, let there exist a set \mathcal{X}_{ot} such that for all $\mathbf{X} \in \mathcal{X}_{\text{ot}}$,*

$\mathcal{L}_{\text{jot}}(\mathbf{X}, \mathbf{X}_{\text{zs}}) \leq \epsilon^2$. Then, it must hold that $\mathcal{X}_{\text{pw}} \subseteq \mathcal{X}_{\text{ot}}$.

Proof. We first note that, clearly, according to Eq. 5, $\hat{\gamma} \in \mathcal{U}(\mathbf{a}, \mathbf{b})$ in Eq. 7 is a valid transport map. Accordingly,

$$\underbrace{\sum_{i=1}^n \sum_{j=1}^n \hat{\gamma}_{ij} c(\mathbf{x}^i, \mathbf{x}_{\text{zs}}^j)}_{\mathcal{L}_{\text{pw}}} \geq \underbrace{\min_{\gamma \in \mathcal{U}(\mathbf{a}, \mathbf{b})} \sum_{i=1}^n \sum_{j=1}^n \gamma_{ij} c(\mathbf{x}^i, \mathbf{x}_{\text{zs}}^j)}_{\mathcal{L}_{\text{jot}}} \quad (8)$$

This is due to \mathcal{L}_{jot} minimizes over all valid transport plans while \mathcal{L}_{pw} is applying one certain valid transport plans that not necessarily is the optimal one. Therefore, given \mathbf{X} , if $\mathcal{L}_{\text{pw}}(\mathbf{X}, \mathbf{X}_{\text{zs}}) \leq \epsilon^2$ holds, $\mathcal{L}_{\text{jot}}(\mathbf{X}, \mathbf{X}_{\text{zs}}) \leq \epsilon^2$ must hold. Hence, any $\mathbf{X} \in \mathcal{X}_{\text{pw}}$ satisfies the condition for \mathcal{X}_{ot} . \square

Now, we will link this theorem to the feasible parameter space of the learnable prompt tokens. First, we recap the objective function with consistency constraints:

$$\min_{\mathcal{P}, \mathcal{Q}} \mathcal{L}_{\text{ce}} + \lambda R(\mathbf{X}, \mathbf{X}_{\text{zs}}), \quad (9)$$

where \mathcal{L}_{ce} denotes the cross-entropy loss widely used in adaptation for CLIP. $\mathcal{P} = \{\mathbf{P}^l\}_{l \in \mathcal{S}_{\text{vision}}}, \mathcal{Q} = \{\mathbf{Q}^l\}_{l \in \mathcal{S}_{\text{text}}}$ denote all learnable tokens from different layers. $\lambda \geq 0$ is a tuning hyperparameter. This objective can be considered as the generalized Lagrange function of the following optimization problem:

$$\min_{\mathcal{P}, \mathcal{Q}} \mathcal{L}_{\text{ce}} \quad \text{s.t. } R(\mathbf{X}, \mathbf{X}_{\text{zs}}) - \epsilon^2 \leq 0, \quad (10)$$

where ϵ^2 is a certain constant. Now, we have the following conclusion:

Theorem 1. Let any Ω_{pw} be a feasible domain of $(\mathcal{P}, \mathcal{Q})$ to the optimization problem defined in Eq. 10 under the point-wise constraint \mathcal{L}_{pw} (i.e., with $R := \mathcal{L}_{\text{pw}}$). Similarly, let any Ω_{ot} be a feasible domain of $(\mathcal{P}, \mathcal{Q})$ to Eq. 10 under the optimal transport constraint \mathcal{L}_{jot} (i.e., with $R := \mathcal{L}_{\text{jot}}$). Then, the following inclusion holds:

$$\Omega_{\text{pw}} \subseteq \Omega_{\text{jot}}. \quad (11)$$

Proof. We define the functions $g_{\text{pw}} : \Omega_{\text{pw}} \rightarrow \mathcal{X}_{\text{pw}}^*$ and $g_{\text{jot}} : \Omega_{\text{ot}} \rightarrow \mathcal{X}_{\text{ot}}^*$ to represent the forward propagation of the model with dataset \mathcal{D} under the point-wise constraint and the optimal transport constraint, respectively.

Now, consider any $(\mathcal{P}, \mathcal{Q}) \in \Omega_{\text{pw}}$. Its representation distribution $\mathbf{X} = g_{\text{pw}}(\mathcal{P}, \mathcal{Q}; \mathcal{D})$ must satisfy

$$\mathcal{L}_{\text{pw}}(\mathbf{X}, \mathbf{X}_{\text{zs}}) \leq \epsilon^2.$$

According to Lemma 1, any $\mathbf{X} \in \mathcal{X}_{\text{pw}}^*$ also satisfies

$$\mathcal{L}_{\text{jot}}(\mathbf{X}, \mathbf{X}_{\text{zs}}) \leq \epsilon^2.$$

This implies that any $\mathbf{X} \in \mathcal{X}_{\text{pw}}^*$ also belongs to the set $\mathcal{X}_{\text{ot}}^*$.

Since for any $\mathbf{X} \in \mathcal{X}_{\text{ot}}^*$, we can find at least one corresponding $(\mathcal{P}, \mathcal{Q}) \in \Omega_{\text{ot}}$, it follows that $\Omega_{\text{pw}} \subseteq \Omega_{\text{jot}}$. \square

Remark 1. Theorem 1 immediately suggests that using optimal transport constraints allows a broader feasible parameter domain of learnable tokens $(\mathcal{P}, \mathcal{Q})$. A larger feasible domain often indicates there are potentially more local minima existing and provides more pathways for the optimizer to explore, which increases the chances of finding a better solution and alleviates a heavy hyperparameter search, i.e., a uniform hyperparameter can achieve reasonable performance across different datasets.

3.4. Training and Inference

Training. Now we assemble the proposed loss in training, which is presented as

$$\min \mathcal{L}_{\text{ce}} + \lambda \mathcal{L}_{\text{jot}}(\mathbf{X}, \mathbf{X}_{\text{zs}}). \quad (12)$$

We employ mini-batch OT to take the mini-batch training nature, which involves computing OT distance within each batch. It is noteworthy that the mini-batch is well-bounded as studied by multiple literatures, including [6, 26, 27].

Inference. Inference does not require any computation of OT and does not need the zero-shot CLIP model. Only the adapted CLIP model is used.

4. Experiment

4.1. Setups

We follow the experimental setups of [16, 41, 44] and evaluate on three tasks: Base-to-Novel Generalization, Cross-Data Evaluation, and Domain Generalization. **For Base-to-Novel Generalization**, we train on base classes and evaluate on both base and novel classes. Following [17], we use 11 datasets. To ensure fairness, we adopt two strategies: using the same epoch for all datasets (adhering to prior methods) and searching for the best epoch on each dataset (as a reference, only to show our method's full potential). **For Cross-Data Evaluation**, we train on ImageNet [5] and test on 10 other datasets without extra fine-tuning. **For Domain Generalization**, we again train on ImageNet [5] and evaluate on four out-of-distribution datasets. Please refer to Appendix A for more details.

Baselines. Despite compared with original CLIP [30], we select multiple recent prompt learning methods for comparison, including: CoOp [44], CoCoOp [43], ProDA [22],

Table 1. **Comparison with state-of-the-art methods on base-to-novel generalization.** The best accuracies are bolded. HM indicates the harmonic mean. Prompt-OT^\dagger represents the best accuracy achieved across different datasets by searching over epochs. It is not intended for direct comparison but is included here for reference. Wilcoxon signed-rank test is shown in Appendix B.

(a) Average			(b) ImageNet			(c) Caltech101			(d) OxfordPets		
	Base	Novel	HM		Base	Novel	HM		Base	Novel	HM
CLIP	69.34	74.22	71.70	CLIP	72.43	68.14	70.22	CLIP	96.84	94.00	95.40
CoOp	82.69	63.22	71.66	CoOp	76.47	67.88	71.92	CoOp	98.00	89.81	93.73
Co-CoOp	80.47	71.69	75.83	Co-CoOp	75.98	70.43	73.10	Co-CoOp	97.96	93.81	95.84
ProGrad	82.48	70.75	76.16	ProGrad	77.02	66.66	71.46	ProGrad	98.02	93.89	95.91
KgCoOp	80.73	73.60	77.00	KgCoOp	75.83	69.96	72.78	KgCoOp	97.72	94.39	96.03
MaPLe	82.28	75.14	78.55	MaPLe	76.66	70.54	73.47	MaPLe	97.74	94.36	96.02
PromptSRC	84.26	76.10	79.97	PromptSRC	77.60	70.73	74.01	PromptSRC	98.10	94.03	96.02
ProDA	81.56	72.30	76.65	ProDA	75.40	70.23	72.72	ProDA	98.27	93.23	95.68
PLOT	83.98	71.72	77.37	PLOT	77.30	69.87	73.40	PLOT	98.53	92.80	95.58
TCP	84.13	75.36	79.51	TCP	77.27	69.87	73.38	TCP	98.23	94.67	96.42
QMaPLe	83.02	75.57	79.12	QMaPLe	76.93	70.73	73.70	QMaPLe	97.97	95.00	96.46
Prompt-OT	84.81	76.25	80.30	Prompt-OT	77.90	69.83	73.65	Prompt-OT	98.37	94.50	96.39
Prompt-OT †	84.82	76.63	80.52	Prompt-OT †	77.63	70.13	73.69	Prompt-OT †	98.33	94.90	96.59
(e) StanfordCars			(f) Flowers102			(g) Food101			(h) FGVCaircraft		
	Base	Novel	HM		Base	Novel	HM		Base	Novel	HM
CLIP	63.37	74.89	68.65	CLIP	72.08	77.80	74.83	CLIP	90.10	91.22	90.66
CoOp	78.12	60.40	68.13	CoOp	97.60	59.67	74.06	CoOp	88.33	82.26	85.19
Co-CoOp	70.49	73.59	72.01	Co-CoOp	94.87	71.75	81.71	Co-CoOp	90.70	91.29	90.99
ProGrad	77.68	68.63	72.88	ProGrad	95.54	71.87	82.03	ProGrad	90.37	89.59	89.98
KgCoOp	71.76	75.04	73.36	KgCoOp	95.00	74.73	83.65	KgCoOp	90.50	91.70	91.09
MaPLe	72.94	74.00	73.47	MaPLe	95.92	72.46	82.56	MaPLe	90.71	92.05	91.38
PromptSRC	78.27	74.97	76.58	PromptSRC	98.07	76.50	85.95	PromptSRC	90.67	91.53	91.10
ProDA	74.70	71.20	72.91	ProDA	97.70	68.68	80.66	ProDA	90.30	88.57	89.43
PLOT	79.07	74.80	76.88	PLOT	97.93	73.53	83.99	PLOT	89.80	91.37	90.58
TCP	80.80	74.13	77.32	TCP	97.73	75.57	85.23	TCP	90.57	91.37	90.97
QMaPLe	75.00	73.67	74.33	QMaPLe	96.43	74.33	83.95	QMaPLe	90.63	92.10	91.36
Prompt-OT	80.60	74.80	77.59	Prompt-OT	98.17	77.03	86.32	Prompt-OT	90.67	91.63	91.15
Prompt-OT †	81.17	74.70	77.80	Prompt-OT †	98.23	77.53	86.66	Prompt-OT †	90.70	92.00	91.35
(i) SUN397			(j) DTD			(k) EuroSAT			(l) UCF101		
	Base	Novel	HM		Base	Novel	HM		Base	Novel	HM
CLIP	69.36	75.35	72.23	CLIP	53.24	59.90	56.37	CLIP	56.48	64.05	60.03
CoOp	80.60	65.89	72.51	CoOp	79.44	41.18	54.24	CoOp	92.19	54.74	68.69
Co-CoOp	79.74	76.86	78.27	Co-CoOp	77.01	56.00	64.85	Co-CoOp	87.49	60.04	71.21
ProGrad	81.26	74.17	77.55	ProGrad	77.35	52.35	62.45	ProGrad	90.11	60.89	72.67
KgCoOp	80.29	76.53	78.36	KgCoOp	77.55	54.99	64.35	KgCoOp	85.64	64.34	73.48
MaPLe	80.82	78.70	79.75	MaPLe	80.36	59.18	68.16	MaPLe	94.07	73.23	82.35
PromptSRC	82.67	78.47	80.52	PromptSRC	83.37	62.97	71.75	PromptSRC	92.90	73.90	82.32
ProDA	78.67	76.93	77.79	ProDA	80.67	56.48	66.44	ProDA	83.90	66.00	73.88
PLOT	82.20	73.63	77.68	PLOT	81.97	43.80	57.09	PLOT	93.70	62.67	75.11
TCP	82.63	78.20	80.35	TCP	82.77	58.07	68.25	TCP	91.63	74.73	82.32
QMaPLe	81.33	78.27	79.77	QMaPLe	80.77	57.63	67.27	QMaPLe	94.30	79.47	86.25
Prompt-OT	82.53	78.90	80.68	Prompt-OT	83.63	64.00	72.51	Prompt-OT	93.10	75.27	83.21
Prompt-OT †	82.67	78.90	80.74	Prompt-OT †	83.5	64.27	72.63	Prompt-OT †	92.77	77.10	84.19

MaPLe [16], ProGrad [17], PromptSRC [17], PLOT [2], TCP [41], and QMaPLe/QCoOP [11]. It is worth mentioning that a portion of the methods are only designed for partial tasks, while our method does not have any obstacles to implementation for all tasks. *For the sake of a fair comparison and proof of concept, we will skip comparing methods that introduce substantial additional knowledge (e.g., LLMs or extra larger CLIP models for knowledge distillation) in our main experiments, such as those proposed in [21, 34, 38, 46].*

Implementation details. For fair comparison, we use a ViT-B/16-based CLIP model, consistent with prior work [16, 17, 41]. Prompts are initialized from a normal distribution, except for the text prompts in the text input, which begin with the embedding of "a photo of". We fix the learning rate at 0.005 and set $\lambda = 10$ for all benchmarks. *All reported results are the average of three runs, without any extra augmentation.* Baseline results are taken from their respective papers. For more details, refer to Appendix A.

Table 2. Performance of PromptOT on cross-dataset evaluation and its comparison to existing methods. Here, the model is trained on the ImageNet dataset and evaluated on ten other datasets in a zero-shot setting.

	Caltech	Pets	Cars	Flowers	Food	Aircraft	SUN397	DTD	EuroSAT	UCF	Ave.
CoOp	93.70	89.14	64.51	68.71	85.30	18.47	64.15	41.92	46.39	66.55	63.88
Co-CoOp	94.43	90.14	65.32	71.88	86.06	22.94	67.36	45.73	45.37	68.21	65.74
MaPLe	93.53	90.49	65.57	72.23	86.20	24.74	67.01	46.49	48.06	68.69	66.30
PromptSRC	93.60	90.25	65.70	70.25	86.15	23.90	67.10	46.87	45.50	68.75	65.81
PLOT	92.07	90.10	65.70	69.23	86.23	25.00	61.67	38.60	47.83	67.00	64.34
TCP	93.97	91.25	64.69	71.21	86.69	23.45	67.12	44.35	51.45	68.73	66.29
QCoOp	94.07	90.53	65.97	71.33	86.23	22.73	66.80	44.20	48.23	69.17	65.93
Prompt-OT	94.03	90.47	65.87	71.27	86.43	23.63	67.20	46.67	50.57	69.03	66.52

Table 3. Performance on domain generalization. These baseline models are trained on ImageNet and evaluated on four out-of-distribution ImageNet datasets.

	ImNetV2	ImNetS	ImNetA	ImNetR	Ave.
CLIP	60.83	46.15	47.77	73.96	57.17
UPT	64.35	48.66	50.66	76.24	59.98
CoOp	64.20	47.99	49.71	75.21	59.28
Co-CoOp	64.07	48.75	50.63	76.18	59.90
ProGrad	64.73	47.61	49.39	74.58	59.07
KgCoOp	64.10	48.97	50.69	76.70	60.11
MaPLe	64.07	49.15	50.90	76.98	60.26
PromptSRC	64.35	49.55	50.90	77.80	60.65
TCP	64.60	49.50	51.20	76.73	60.51
QCoOp	63.87	48.93	51.10	76.90	60.20
Prompt-OT	64.35	49.40	51.63	77.40	60.70

4.2. Main Results

Base-to-Novel Generalization. As shown in Table 1, our method significantly outperforms zero-shot CLIP, confirming its effectiveness. In particular, we achieve gains of 15.47%, 2.03%, and 8.60% in base task accuracy, novel task accuracy, and their harmonic mean, respectively. More importantly, when averaged over 11 datasets, our approach surpasses all recent baselines. Specifically, it achieves 84.81% (base task accuracy), 76.26% (novel task accuracy), and 80.30% (harmonic mean), which is an improvement of 0.55%, 0.15%, and 0.33% over the previous state-of-the-art, PromptSRC.

Cross-Dataset Evaluation. Table 2 shows that our method attains an average accuracy of 66.52% across 11 datasets, outperforming all baselines and exceeding PromptSRC by 0.62%.

Domain Generalization. As shown in Table 3, we observe that our method achieves the highest average accuracy on four out-of-distribution datasets.

Overall, our method demonstrates robust performance across three key evaluations. In the base-to-novel generalization setup, it substantially outperforms zero-shot CLIP

and surpasses the previous state-of-the-art in base accuracy, novel accuracy, and harmonic mean. In cross-dataset evaluation and in domain generalization, our method obtains the best overall accuracy without relying on prompt ensembles or text augmentation, underscoring both its effectiveness and simplicity.

5. Analysis

In this section, we will delve into a more detailed analysis of our proposed method. All experiments will be conducted consistently with the setups of base-to-novel generalization. For fairness, we exclude all other components and only apply regularization on the IVLP.

Ours VS Point-wise Constraints. To illustrate the superiority of the proposed method over point-wise constraints, we evaluate it against several baselines: (i) naive L_2 constraints between \mathbf{X} and \mathbf{X}_{zs} with the same regularization strength λ , (ii) **Adaptor-Cos** [34], which introduces adapters at the end of the adapted encoders and employs cosine similarity as the point-wise constraint between representations, (iii) **SRC** [17], which applies L_1 losses for vision and text representations separately and a KL-divergence between prediction probabilities for each instance. (iv) **Separate OT** (see Appendix A), which applies OT-loss for vision and text representations separately. *For a fair comparison, we exclude all additional augmentations, such as ensemble techniques and LLM-based augmentation.* Table 4 reports both the performance metrics and the corresponding statistical test results. Our primary observation is that all these methods achieve a better balance between novel and base tasks than the model without any constraints, with a minimum improvement of 1.83% in harmonic mean accuracy. More importantly, the OT-based methods outperform all recent approaches based on point-wise constraints. Even without joint representation, applying OT for two domains separately can outperform all other point-wise methods. Additionally, compared to SRC, the previ-

Table 4. Comparison of performance with point-wise constraints. Reported p -values are obtained from Wilcoxon signed-rank tests comparing the baseline and our method.

Reg. Method	Base	Novel	HM	$p < 0.05$
w/o Constraints	84.20	71.21	77.16	✓
Point-wise	L_2 between X, X_{zs}	84.20	74.68	79.16
	Adaptor-Cos	83.12	75.25	78.99
	<i>From CoPrompt [34]</i>			✓
	SRC	84.41	74.89	79.37
	<i>From PromptSRC [17]</i>			✓
	Separate OT	84.50	75.48	79.74
Ours	84.81	76.25	80.30	—

Table 5. Ablation study on different modalities for imposing constraints.

Text	Vision	Scheme	Base	Novel	HM
✗	✗	-	84.20	71.21	77.16
✓	✗	-	84.92	71.75	77.78
✗	✓	-	84.12	72.94	78.12
✓	✓	Separate	84.50	75.48	79.74
✓	✓	Joint	84.81	76.25	80.30

ous state-of-the-art method, our proposed method achieved statistically significant gains of 0.4%, 1.35%, and 0.93% in base task accuracy, novel task accuracy, and harmonic mean accuracy, respectively. Compared to L_2 constraints, we observe that with the same regularization strength λ , L_2 constraints, while preserving good generalizability to novel tasks, fail to yield any improvements on the base task. This suggests that L_2 constraints may be overly restrictive for model adaptation. In contrast, our proposed approach effectively balances performance across both the base and novel tasks, demonstrating that modeling cross-instance correlation while allowing the model greater flexibility in updating leads to an optimal trade-off, as expected in Fig. 1.

Effectiveness of Joint Representation. Here, we investigate alternative approaches to imposing constraints between zero-shot and adapted representations. Specifically, we examine four different strategies: (i) imposing the constraint solely on the text representation, (ii) imposing the constraint solely on the vision representation, (iii) applying constraints separately to text and vision representation distributions (i.e., Separate OT), and (iv) our proposed joint representation, which considers an instance includes both vision and text representations.

As shown in Table 5, applying constraints to both modalities yields a significantly greater improvement (2.58% and 3.14% in HM) compared to imposing the constraint on a

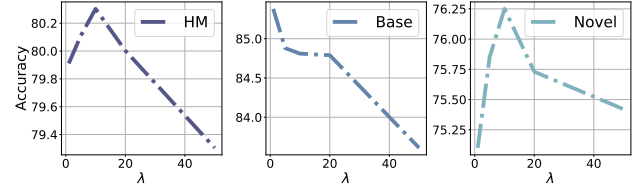


Figure 2. The effectiveness of λ on base-to-novel generalization tasks averaged over 11 datasets.

single modality (0.62% and 0.96% in HM). Moreover, our proposed joint representation yields greater improvements compared to applying constraints separately on vision and text distributions, which potentially results in unbalanced constraint strength. Our method leads to the highest increase in HM (3.14%), suggesting that it provides the most effective balance between minimizing errors in both novel and base classes.

Sensitivity of λ . We further conduct a study to evaluate the impact of different values of λ on adaptation. As shown in Fig. 2, as λ increases, the constraints become stronger, leading to a decline in adaptation to the base class. Meanwhile, the accuracy on the novel class initially increases before decreasing, indicating that the zero-shot weights may not be optimal for both novel and base tasks. This suggests that some relaxation is necessary to achieve a well-balanced trade-off. Excessively strong constraints may prevent the model from reaching the low-error regions of both tasks in the optimization landscape. Empirically, we find that $\lambda = 10$ achieves a good balance between generalization and adaptation.

Efficiency. Our method introduces only a minor computational overhead during training, as shown in Table 6, incurring approximately a 1.8% increase in runtime with negligible additional GPU usage.

Table 6. Comparison of Computational Cost.

	Runtime	GPU
w/o Constraint	0.0385s/step	3948MB
Ours	0.0392s/step	3950MB

6. Conclusion

In this work, we proposed an Optimal Transport (OT) Regularization framework for vision-language prompt learning to mitigate forgetting and enhance adaptability. Unlike rigid point-wise constraints, our method uses OT to model cross-instance relationships and preserve the embedding struc-

ture between pre-trained and fine-tuned models. Theoretical analysis shows that OT constraints offer a broader feasible parameter space, enabling more robust prompt learning. Extensive experiments demonstrate that our approach outperforms state-of-the-art methods across various generalization settings. Future directions include incorporating adaptive regularization strength to improve trade-offs dynamically and exploring efficient transport solvers for broader applications.

References

- [1] Lukas Bossard, Matthieu Guillaumin, and Luc Van Gool. Food-101-mining discriminative components with random forests. In *ECCV*, pages 446–461. Springer, 2014. [10](#)
- [2] Guangyi Chen, Weiran Yao, Xiangchen Song, Xinyue Li, Yongming Rao, and Kun Zhang. PLOT: Prompt learning with optimal transport for vision-language models. In *The Eleventh International Conference on Learning Representations*, 2023. [2, 3, 6](#)
- [3] Mircea Cimpoi, Subhransu Maji, Iasonas Kokkinos, Sammy Mohamed, and Andrea Vedaldi. Describing textures in the wild. In *CVPR*, pages 3606–3613, 2014. [10](#)
- [4] Janez Demšar. Statistical comparisons of classifiers over multiple data sets. *The Journal of Machine learning research*, 7:1–30, 2006. [11](#)
- [5] Jia Deng, Wei Dong, Richard Socher, Li-Jia Li, Kai Li, and Li Fei-Fei. Imagenet: A large-scale hierarchical image database. In *CVPR*, pages 248–255. Ieee, 2009. [5, 10](#)
- [6] Kilian Fatras, Younes Zine, Szymon Majewski, Rémi Flamary, Rémi Gribonval, and Nicolas Courty. Minibatch optimal transport distances: analysis and applications. *arXiv preprint arXiv:2101.01792*, 2021. [5](#)
- [7] Li Fei-Fei, Rob Fergus, and Pietro Perona. Learning generative visual models from few training examples: An incremental bayesian approach tested on 101 object categories. In *CVPR Workshop*, pages 178–178. IEEE, 2004. [10](#)
- [8] Chengjian Feng, Yujie Zhong, Zequn Jie, Xiangxiang Chu, Haibing Ren, Xiaolin Wei, Weidi Xie, and Lin Ma. Promptdet: Towards open-vocabulary detection using uncurated images. In *ECCV*, 2022. [1](#)
- [9] Chun-Mei Feng, Kai Yu, Yong Liu, Salman Khan, and Wangmeng Zuo. Diverse data augmentation with diffusions for effective test-time prompt tuning. In *Proceedings of the IEEE/CVF International Conference on Computer Vision*, pages 2704–2714, 2023. [3](#)
- [10] Peng Gao, Shijie Geng, Renrui Zhang, Teli Ma, Rongyao Fang, Yongfeng Zhang, Hongsheng Li, and Yu Qiao. Clip-adapter: Better vision-language models with feature adapters. *International Journal of Computer Vision*, 132(2): 581–595, 2024. [2](#)
- [11] Tianxiang Hao, Xiaohan Ding, Juxiao Feng, Yuhong Yang, Hui Chen, and Guiguang Ding. Quantized prompt for efficient generalization of vision-language models. In *European Conference on Computer Vision*, pages 54–73. Springer, 2025. [2, 6](#)
- [12] Patrick Helber, Benjamin Bischke, Andreas Dengel, and Damian Borth. Eurosat: A novel dataset and deep learning benchmark for land use and land cover classification. *J-STARS*, 12(7):2217–2226, 2019. [10](#)
- [13] Dan Hendrycks, Steven Basart, Norman Mu, Saurav Kadavath, Frank Wang, Evan Dorundo, Rahul Desai, Tyler Zhu, Samyak Parajuli, Mike Guo, et al. The many faces of robustness: A critical analysis of out-of-distribution generalization. In *ICCV*, pages 8340–8349, 2021. [10](#)
- [14] Dan Hendrycks, Kevin Zhao, Steven Basart, Jacob Steinhardt, and Dawn Song. Natural adversarial examples. In *CVPR*, pages 15262–15271, 2021. [10](#)
- [15] Chao Jia, Yafei Yang, Ye Xia, Yi-Ting Chen, Zarana Parekh, Hieu Pham, Quoc Le, Yun-Hsuan Sung, Zhen Li, and Tom Duerig. Scaling up visual and vision-language representation learning with noisy text supervision. In *ICML*, pages 4904–4916. PMLR, 2021. [1](#)
- [16] Muhammad Uzair Khattak, Hanoona Rasheed, Muhammad Maaz, Salman Khan, and Fahad Shahbaz Khan. Maple: Multi-modal prompt learning. In *CVPR*, pages 19113–19122, 2023. [2, 3, 4, 5, 6](#)
- [17] Muhammad Uzair Khattak, Syed Talal Wasim, Muzammal Naseer, Salman Khan, Ming-Hsuan Yang, and Fahad Shahbaz Khan. Self-regulating prompts: Foundational model adaptation without forgetting. In *Proceedings of the IEEE/CVF International Conference on Computer Vision*, pages 15190–15200, 2023. [1, 2, 3, 4, 5, 6, 7, 8, 10](#)
- [18] Konwoo Kim, Michael Laskin, Igor Mordatch, and Deepak Pathak. How to adapt your large-scale vision-and-language model, 2022. [1](#)
- [19] James Kirkpatrick, Razvan Pascanu, Neil Rabinowitz, Joel Veness, Guillaume Desjardins, Andrei A Rusu, Kieran Milan, John Quan, Tiago Ramalho, Agnieszka Grabska-Barwinska, et al. Overcoming catastrophic forgetting in neural networks. *Proceedings of the national academy of sciences*, 114(13):3521–3526, 2017. [2, 3](#)
- [20] Jonathan Krause, Michael Stark, Jia Deng, and Li Fei-Fei. 3d object representations for fine-grained categorization. In *ICCV*, pages 554–561, 2013. [10](#)
- [21] Zheng Li, Xiang Li, Xinyi Fu, Xin Zhang, Weiqiang Wang, Shuo Chen, and Jian Yang. Promptkd: Unsupervised prompt distillation for vision-language models. In *Proceedings of the IEEE/CVF Conference on Computer Vision and Pattern Recognition*, pages 26617–26626, 2024. [6](#)
- [22] Yuning Lu, Jianzhuang Liu, Yonggang Zhang, Yajing Liu, and Xinmei Tian. Prompt distribution learning. In *CVPR*, pages 5206–5215, 2022. [5](#)
- [23] Timo Lüddecke and Alexander Ecker. Image segmentation using text and image prompts. In *CVPR*, pages 7086–7096, 2022. [1](#)
- [24] Subhransu Maji, Esa Rahtu, Juho Kannala, Matthew Blaschko, and Andrea Vedaldi. Fine-grained visual classification of aircraft. *arXiv preprint arXiv:1306.5151*, 2013. [10](#)
- [25] Duy MH Nguyen, An T Le, Trung Q Nguyen, Nghiem T Diep, Tai Nguyen, Duy Duong-Tran, Jan Peters, Li Shen, Mathias Niepert, and Daniel Sonntag. Dude: Dual

- distribution-aware context prompt learning for large vision-language model. *arXiv preprint arXiv:2407.04489*, 2024. 3
- [26] Khai Nguyen, Dang Nguyen, Quoc Nguyen, Tung Pham, Hung Bui, Dinh Phung, Trung Le, and Nhat Ho. On transportation of mini-batches: A hierarchical approach. In *Proceedings of the 39th International Conference on Machine Learning*, 2022. 5
- [27] Khai Nguyen, Dang Nguyen, Tung Pham, and Nhat Ho. Improving mini-batch optimal transport via partial transportation. In *Proceedings of the 39th International Conference on Machine Learning*, 2022. 5
- [28] Maria-Elena Nilsback and Andrew Zisserman. Automated flower classification over a large number of classes. In *ICVGIP*, pages 722–729. IEEE, 2008. 10
- [29] Omkar M Parkhi, Andrea Vedaldi, Andrew Zisserman, and CV Jawahar. Cats and dogs. In *CVPR*, pages 3498–3505. IEEE, 2012. 10
- [30] Alec Radford, Jong Wook Kim, Chris Hallacy, Aditya Ramesh, Gabriel Goh, Sandhini Agarwal, Girish Sastry, Amanda Askell, Pamela Mishkin, Jack Clark, et al. Learning transferable visual models from natural language supervision. In *ICML*, pages 8748–8763. PMLR, 2021. 1, 5
- [31] Hanoona Rasheed, Muhammad Uzair Khattak, Muhammad Maaz, Salman Khan, and Fahad Shahbaz Khan. Fine-tuned clip models are efficient video learners. In *CVPR*, pages 6545–6554, 2023. 4
- [32] Benjamin Recht, Rebecca Roelofs, Ludwig Schmidt, and Vaishaal Shankar. Do imagenet classifiers generalize to imagenet? In *ICML*, pages 5389–5400. PMLR, 2019. 10
- [33] Robin Rombach, Andreas Blattmann, Dominik Lorenz, Patrick Esser, and Björn Ommer. High-resolution image synthesis with latent diffusion models. In *Proceedings of the IEEE/CVF conference on computer vision and pattern recognition*, pages 10684–10695, 2022. 3
- [34] Shuvendu Roy and Ali Etemad. Consistency-guided prompt learning for vision-language models. In *The Twelfth International Conference on Learning Representations*, 2024. 2, 3, 6, 7, 8
- [35] Khurram Soomro, Amir Roshan Zamir, and Mubarak Shah. Ucf101: A dataset of 101 human actions classes from videos in the wild. *arXiv preprint arXiv:1212.0402*, 2012. 10
- [36] Cédric Villani et al. *Optimal transport: old and new*. Springer, 2009. 4
- [37] Haohan Wang, Songwei Ge, Zachary Lipton, and Eric P Xing. Learning robust global representations by penalizing local predictive power. In *NeurIPS*, 2019. 10
- [38] Ge Wu, Xin Zhang, Zheng Li, Zhaowei Chen, Jiajun Liang, Jian Yang, and Xiang Li. Cascade prompt learning for vision-language model adaptation. In *European Conference on Computer Vision*, pages 304–321. Springer, 2025. 6
- [39] Jianxiong Xiao, James Hays, Krista A Ehinger, Aude Oliva, and Antonio Torralba. Sun database: Large-scale scene recognition from abbey to zoo. In *CVPR*, pages 3485–3492. IEEE, 2010. 10
- [40] Lingxiao Yang, Ru-Yuan Zhang, Yanchen Wang, and Xiaohua Xie. Mma: Multi-modal adapter for vision-language models. In *Proceedings of the IEEE/CVF Conference on Computer Vision and Pattern Recognition*, pages 23826–23837, 2024. 2
- [41] Hantao Yao, Rui Zhang, and Changsheng Xu. Tcp: Textual-based class-aware prompt tuning for visual-language model. In *Proceedings of the IEEE/CVF Conference on Computer Vision and Pattern Recognition*, pages 23438–23448, 2024. 2, 3, 5, 6
- [42] Renrui Zhang, Wei Zhang, Rongyao Fang, Peng Gao, Kun-chang Li, Jifeng Dai, Yu Qiao, and Hongsheng Li. Tip-adapter: Training-free adaption of clip for few-shot classification. In *European conference on computer vision*, pages 493–510. Springer, 2022. 2
- [43] Kaiyang Zhou, Jingkang Yang, Chen Change Loy, and Ziwei Liu. Conditional prompt learning for vision-language models. In *CVPR*, pages 16816–16825, 2022. 1, 2, 5
- [44] Kaiyang Zhou, Jingkang Yang, Chen Change Loy, and Ziwei Liu. Learning to prompt for vision-language models. *IJCV*, 130(9):2337–2348, 2022. 1, 2, 5
- [45] Beier Zhu, Yulei Niu, Yucheng Han, Yue Wu, and Hanwang Zhang. Prompt-aligned gradient for prompt tuning. In *Proceedings of the IEEE/CVF International Conference on Computer Vision*, pages 15659–15669, 2023. 2, 3
- [46] Yuhang Zhu, Yuyang Ji, Zhiyu Zhao, Gangshan Wu, and Limin Wang. Awt: Transferring vision-language models via augmentation, weighting, and transportation. *arXiv preprint arXiv:2407.04603*, 2024. 3, 6

A. Implementation Detail

We train PromptOT for 30 epochs for the Base-to-Novel Generalization benchmark and 2 epochs for the remaining three benchmark settings, respectively. The respective epochs are fixed across all datasets. All experiments are run on a node of the cluster with one V100 16GB NVIDIA GPU. Following a deep prompting strategy, we apply prompts to all transformer blocks for the first benchmark and the first three transformer blocks for the remaining benchmarks, and we use four text prompts and four vision prompts. Following previous works [17], in For Base-to-Novel Generalization benchmark, we set the first half of classes as base classes and the remaining classes as novel classes. Models are only trained on base classes. The accuracy is reported based on the evaluation of base classes and novel classes, respectively. The overview of this framework is shown in Fig. S3.

A.1. Datasets

We used the following datasets in our experiments:

Exps. 1 and 2. ImageNet [5], Caltech101 [7], Oxford-Pets [29], StanfordCars [20], Flowers102 [28], Food101 [1], and FGVCAircraft [24], SUN397 [39], UCF101 [35], DTD [3], and EuroSAT [12].

Exp. 3. ImageNet [5] as a source dataset and use ImageNet-A [14], ImageNet-R [13], ImageNet-Sketch [37] and ImageNetV2 [32].

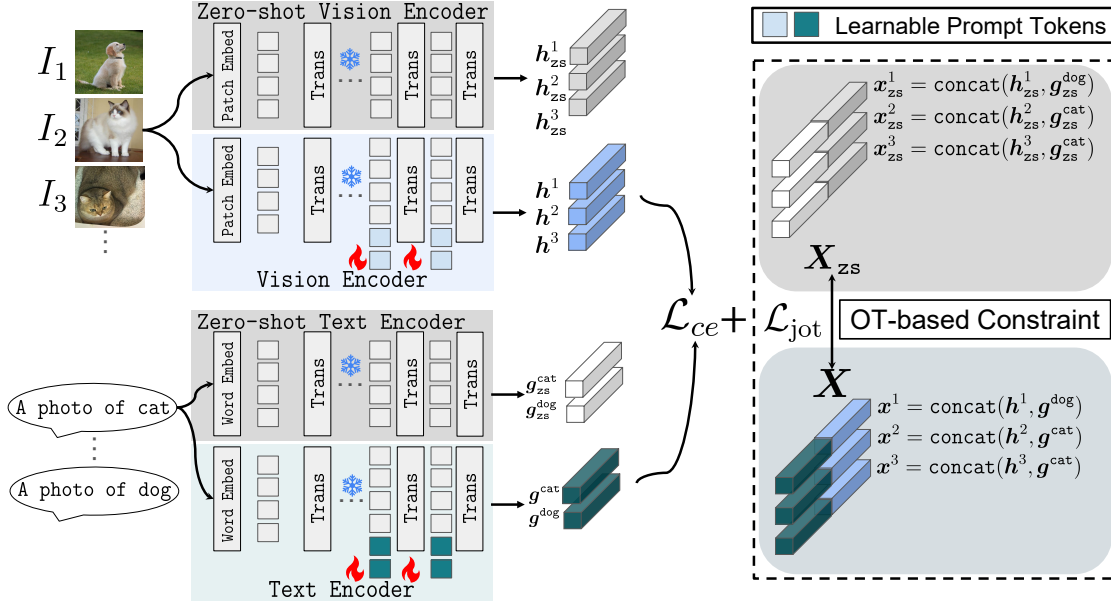


Figure S3. The overview of our proposed framework. Only the prompt tokens are trainable, and the rest of the weights in both the zero-shot encoders and the adapted encoders are frozen. Despite the cross-entropy \mathcal{L}_{ce} adopted, we also adopt the proposed joint optimal transport loss \mathcal{L}_{jot} between joint zero-shot representation and adapted representation to constrain the model.

A.2. Separate OT

The way of applying **separate OT** is similar to SRC loss. Suppose the adapted vision features are presented as $\mathbf{H} = \{\mathbf{h}^i\}_{i=1}^n$ and adapted text features are presented as $\mathbf{G} = \{\mathbf{g}^i\}_{i=1}^C$. Again, n and C denote the number of samples and number of classes, respectively. Similarly, we denote the zero-shot vision features and text features as \mathbf{H}_{zs} and \mathbf{H}_{zs} , respectively. The Separate OT is denoted as:

$$\mathcal{L}_{SOT} = \mathcal{L}_{OT}(\mathbf{H}, \mathbf{H}_{zs}) + \mathcal{L}_{OT}(\mathbf{G}, \mathbf{G}_{zs}). \quad (13)$$

A.3. Reproducibility

The code and model weights will be publicly released upon acceptance. **In the supplementary zip file, we provide the key code for the configuration and implementation of our proposed method.**

Our code is developed based on <https://github.com/muzairkhattak/PromptSRC>.

B. Wilcoxon signed-rank test

We perform a Wilcoxon signed-rank test [4] to compare our method with PromptSRC, the previous state-of-the-art, using harmonic mean accuracy as the evaluation metric. As shown in Table S7, our method achieves statistically significant improvements over PromptSRC (p-value < 0.05).

Table S7. Wilcoxon signed-rank test on Exp 1.

PromptSRC VS Prompt-OT	
P-value	0.016

C. Limitation

While our proposed PromptOT framework demonstrates strong performance across various benchmarks and introduces theoretically grounded improvements over prior prompt learning approaches, we acknowledge certain limitations that open avenues for future exploration:

First, the OT-based regularization introduces additional computational overhead compared to simpler constraints (e.g., point-wise L2 losses). Although we adopt mini-batch OT solvers to keep training efficient, the method still requires access to additional computational resources.

Second, while our approach avoids relying on external augmentations or auxiliary models (e.g., large LLMs), this also means it may not fully leverage certain recent advances in generative or data-enhancement techniques. Integrating such components in a resource-efficient manner could further boost performance.